Short-term fate of intertidal microphytobenthos carbon under enhanced nutrient availability: A ^{13}C pulse-chase experiment

Philip M. Riekenberg[1,a*], Joanne M. Oakes[1], Bradley D. Eyre[1]

[1]Centre for Coastal Biogeochemistry, Southern Cross University, PO Box 157, Lismore, NSW, 2480, Australia

[a]Present address: NIOZ Royal Netherlands Institute for Sea Research, Department of Marine Microbiology and Biogeochemistry, PO Box 59, 1790AB Den Burg

[*] Corresponding author: phrieken@gmail.com, (0031) 222 369 409

Keywords: benthic microalgae, bacteria, biomarker, nutrients

Running head: Intertidal carbon processing

ABSTRACT:

Shallow coastal waters in many regions are subject to nutrient enrichment. Microphytobenthos (MPB) can account for much of the carbon (C) fixation in these environments, depending on the depth of the water column, but the effect of enhanced nutrient availability on the processing and fate of MPB-derived C is relatively unknown. In this study, MPB were labeled (stable isotope enrichment) in situ using ^{13}C-sodium bicarbonate. The processing and fate of the newly-fixed MPB-C was then traced using ex situ incubations over 3.5 d under different concentrations of nutrients (NH_4^+ and PO_4^{3-}: ambient, 2× ambient, 5× ambient, and 10× ambient). After 3.5 d, sediments incubated with increased nutrient concentrations (amended treatments) had increased loss of ^{13}C from sediment organic matter as a portion of initial uptake (95% remaining in ambient vs 79-93% for amended treatments) and less ^{13}C in MPB (52% ambient, 26-49% amended), most likely reflecting increased turnover of MPB-derived C supporting increased production of extracellular enzymes and storage products. Loss of MPB-derived C to the water column via dissolved organic C was minimal regardless of treatment (0.4-0.6%). Loss due to respiration was more substantial, with effluxes of dissolved inorganic C increasing with additional nutrient availability (4% ambient, 6.6-19.8% amended). These shifts resulted in a decreased turnover time for algal C (419 d ambient, 134-199 d amended). This suggests that nutrient enrichment of estuaries may ultimately lead to decreased retention of carbon within MPB-dominated sediments.

1.0 Introduction

Intertidal sediments are important sites for the processing of carbon (C) within estuaries, producing, remineralizing, and transforming considerable amounts of organic material prior to its export to the coastal shelf (Bauer et al. 2013). Algal production is a key source of C within the coastal zone, and is primarily derived from microphytobenthos (MPB) in shallow photic sediments (Hardison et al. 2013; Middelburg et al. 2000). In addition to algal cells being a labile carbon source, MPB exude large amounts of carbohydrates as extracellular polymeric substances (EPS) (Goto et al. 1999) that allow for vertical migration and enhance sediment stability (Stal 2010). A better understanding of the carbon pathways utilized during processing of algal cells and exudates within sediments is important for determining the quality and quantity of carbon exported from estuarine waters to continental shelves.

Application of rare isotope tracers can render fractionation effects and variability that affect natural abundance stable isotope techniques negligible and has been useful for elucidating pathways for the processing and loss of MPB-derived C within estuarine sediments. Loss pathways for MPB-derived C include resuspension (Oakes and Eyre 2014), fluxes of dissolved inorganic C (DIC) due to mineralization and respiration (Evrard et al. 2012; Oakes et al. 2012), fluxes of dissolved organic C (DOC) comprised of microbial exudates and products from cell lysis (Oakes et al. 2010a), and direct production of CO_2 (Oakes and Eyre 2014). Stable isotope tracer studies have also enabled quantification of the trophic transfer (Middelburg et al. 2000; Miyatake et al. 2014; Nordström et al. 2014; Oakes et al. 2010a) and flux of newly produced C from sediments (Andersson et al. 2008; Oakes et al. 2012; Van Nugteren et al. 2009).

When ^{13}C is combined with analysis of phospholipid-linked fatty acids (PLFAs), it becomes possible to trace C transfer into individual microbial groups that account for the living biomass within sediment organic C (OC) (Drenovsky et al. 2004; Hardison et al. 2011; Oakes et al. 2012; Oakes and Eyre 2014; Spivak 2015). This allows for the quantification of microbial transfers of newly produced algal C between MPB and bacteria and the relative contributions of MPB and bacteria to microbial biomass in sediment OC. This technique has shown that EPS produced by MPB is readily utilized as a C source for heterotrophic bacteria (Oakes et al. 2010; van Oevelen et al. 2006; Hardison et al. 2011). Pathways for processing of MPB-derived C have been reasonably well described, but the response of these pathways to local environmental changes remains a significant knowledge gap.

A major source of environmental change in coastal systems is nutrient over-enrichment (Cloern et al. 2001), which may affect the assimilation and flux pathways of MPB-derived carbon through 1) increased microbial biomass or an increase in production of extracellular enzymes resulting from relaxation of nutrient limitation, 2) increased algal production that drives elevated heterotrophic processes as bacteria utilize newly produced C, and 3) increased loss of C as DIC via respiratory pathways as heterotrophic processes dominate. MPB are able to use both porewater and water column nutrients, and although MPB biomass can increase with elevated nutrient availability (Armitage and Fong 2004; Cook et al. 2007), this is not always the case, with multiple studies finding no corresponding increase in MPB biomass (Alsterberg et al. 2012; Pascal et al. 2013; Piehler et al. 2010; Spivak and Ossolinski 2016). Processing and mineralization of C are significantly affected by changes in the relationship between MPB and bacteria (Evrard et al. 2012). Both EPS production and bacterial utilization of newly produced EPS may decrease with increasing nutrient availability

(Cook et al. 2007). Increased autochthonous production driven by nutrient enrichment can lead to increased heterotrophy, as newly produced organic matter is mineralized (Fry et al. 2015), resulting in increased DIC production. Increased remineralization of newly produced MPB-C will result in greater loss of DIC from intertidal sediment via bacterial respiration (Hardison et al. 2011).

In this ^{13}C pulse-chase study we aimed to quantify the short-term effects of increased nutrient concentrations on the processing pathways for MPB-derived C within subtropical intertidal sediments. The in situ MPB community was used to provide a pulse of labeled MPB-C of similar quantity and quality to normal production. Even application of separate label applications for each plot prior to incubation served to isolate the subsequent effect of increased nutrient availability on the processing of MPB-derived C. Pathways considered included transfer through sediment compartments (MPB, bacteria, uncharacterized and sediment OC), and loss via fluxes of DOC and DIC. We expected increased nutrient availability to stimulate production of MPB-C after initial labeling, resulting in decreased turnover times for MPB-C as well as a shift towards dominance of heterotrophic processes as bacteria utilize this additional labile C. We further hypothesized that enhanced heterotrophy would increase loss of newly fixed algal-derived C via respiration as $DI^{13}C$. Incorporation of ^{13}C into biomarkers should reflect the shift towards heterotrophy, with quicker shifts towards increased bacterial utilization of newly produced algal C corresponding with increased nutrient load. Both DIC and DOC should be significant loss pathways for newly produced algal C as labile OM is readily processed by heterotrophs.

2.0 Methods

2.1 Study site

The study site was a subtropical intertidal shoal ~ 2 km upstream of the mouth of the Richmond River estuary in New South Wales, Australia (28˚52'30"S, 153˚33'26"E). The 6900 km^2 catchment has an annual rainfall of 1300 mm (McKee et al. 2000) and an average flow rate of 2200 ML d^{-1} (daily gauged flow adjusted for catchment area, averaged over years for which data was available; 1970–2013). Although the Richmond River Estuary has highly variable flushing, salinity, and nutrient concentrations associated with frequent episodic rainfall events and flooding (Eyre 1997; Mckee et al. 2000), this study was undertaken during a dry period. The site experiences semidiurnal tides with a range of ~2 m. Samples were collected in summer January 2015 with average site water temperature of 25.6 ± 2.3°C. Sediment at depths of 0-2 cm, 2-5 cm and 5-10 cm was dominated by fine sand (66%-73%), and sediment across 0-10 cm had an organic C content of 17.5 ± 0.02 mol C m^{-2}. Sediment molar C:N was lowest at 2-5 cm, but comparable across all other depths (top scrape (TS) 14.4 ± 1.6, 0.13± 0.02 %OC; 0-2 cm 17.2 ± 1.7, 0.18± 0.07 %OC; 2-5 cm 10.9 ± 0.5, 0.23± 0.06 %OC; 5-10 cm 16.2 ± 2.2, 0.14± 0.03 %OC).

2.2 Overview

We labeled MPB with ^{13}C via in situ application of ^{13}C-labeled sodium bicarbonate to exposed intertidal sediments. Unincorporated ^{13}C was flushed from the sediment during the next tidal inundation of the site. Sediment cores were collected and incubated in the laboratory over 3.5 d under four nutrient enrichment scenarios (ambient, minimal, moderate, and elevated) using pulsed nutrient additions. Incubation of cores ex situ allowed for explicit control of nutrient additions and examination of the short-term processing and fate (loss to overlying water) of MPB carbon. Sediments remained inundated during incubations with

minimal water exchange, as might be expected during neap tide at this site. Inundation also served to minimize C loss via physical resuspension and export while we were examining sediment processing.

2.3 ^{13}C-labeling

Bare sediment within a 2 m^2 experimental plot was ^{13}C-labeled when sediments were first exposed during the ebbing tide in the middle of the day by using motorized sprayers to evenly apply 99% $NaH^{13}CO_3$ onto individual 400 cm^2 subplots, closely following the method outlined in Oakes and Eyre (2014). Label applications were prepared using NaCl-amended Milli-Q matching site salinity (34.6), and 20 ml aliquots (1.7 mmol ^{13}C) were applied to each individual subplot, resulting in application of 42.5 mmol ^{13}C m^{-2}. The use of individual aliquots of label ensured even ^{13}C application across the sediment surface. Assimilation of label by the sediment community occurred over ~4 hours with average light exposure of 1376 µE m^{-2} s^{-1}, before tidal inundation removed the majority of unincorporated ^{13}C. Removal was confirmed by loss of 99.0% of the applied ^{13}C from treatment applications within initial cores sampled in the field.

2.4 Collection of sediment cores

Prior to label application, 3 cores (9 cm diameter, 20 cm depth) were collected from unlabeled sediment surrounding the treatment plots and immediately extruded and sectioned (0-0.2 cm (top scrape, TS), 0.2-2 cm, 2-5 cm, and 5-10 cm) to provide control natural abundance sediment OC δ^{13}C values for sediment depths within the study site. Eleven hours after label application, at low tide, 35 sediment cores were similarly collected from the labeled plot using Plexiglas core liners. Immediately, three cores were extruded and sectioned as above to determine initial ^{13}C uptake and grain size distribution for all sediment depths, and

chlorophyll-*a* (Chl-*a*) concentrations in 0-1 cm sediments. All samples were placed within plastic zip-lock bags, transported to the laboratory on ice, and stored frozen in the dark (-20 ˚ C). Plexiglas plates were used to seal the bottom of the core liners, and cores for incubation were then transported to the laboratory within 2 hours of sampling. Site water (400 L) was collected and transported to the laboratory for use in incubations.

2.5 Nutrient amendment

Pulsed applications of nutrients for each treatment amendment were used to mimic a range of nutrient concentrations without exceeding sediment capacity for uptake. The treatment tanks were set up at ambient concentration (site water, DIN of 2.5 ± 0.04 µmol N L^{-1}, measured on incoming tide), and with N (NH_4^+) and P (H_3PO_4) amendment to unfiltered site water at 2× (minimal treatment), 5× (moderate treatment) and 10× (elevated treatment) average water column concentrations near the study site (4 µmol L^{-1} NH_4^+ and 5 µmol L^{-1} PO_4^{3-}; Eyre (1997; 2000). To allow thorough mixing, the initial pulse of nutrients was added to both incubation tanks and bags holding replacement water for sampling, one hour prior to cores being transferred into the incubation tanks. An additional pulse of NH_4^+ was applied to incubation tanks at 1.5 d (after sample collection) to mimic the nutrient availability that occurs with regular inundation of tidal sediments. Silica (Si) was also added to all incubation tanks at 2.5 d (after sample collection) to ensure that isolation of the benthic diatom-dominated sediment from regular water turnover did not result in secondary limitation of Si. There was no significant accumulation of NH_4^+ within treatment tank water, as nutrients were readily processed (Supplemental Fig. 1). Processing of newly fixed MPB-C occurred in the 13 h prior to incubation with nutrient amendments, but was likely similar across cores as they were kept in identical conditions prior to incubation before random allocation to treatments. Although

MPB-C was not freshly fixed at 13 h and likely more refractory as a result, the available C was still relatively labile and readily processed across all treatments.

2.6 Benthic flux incubations

In the laboratory, cores were fitted with magnetic stir bars positioned 10 cm above the sediment surface, filled with ~2 L of site water, and randomly allocated to one of the four 85 L treatment tanks (Ambient, Minimal, Moderate, Elevated; eight cores per treatment). Water in the treatment tanks and cores was continuously recirculated, held at in situ temperature (25 ± 1^{o}C) by a chiller on each tank, and aerated. Cores were stirred via a rotating magnet at the center of each treatment tank, which interacted with the magnetic stir bars. Stirring occurred at a rate below the threshold for sediment resuspension (Ferguson et al. 2003). Three sodium halide lamps suspended above the treatment tanks provided 824 ± 40 µE m^{-2} s^{-1} to the sediment/water interface within the cores on a 12 h light/12 h dark cycle which approximated the average light level measured at the sediment surface during inundation (941.4 ± 139 µE m^{-2} s^{-1}). Cores were allowed to acclimate in tanks for 6 h prior to the start of incubation to allow for the re-establishment of microclimates and anaerobic zonation that was potentially disturbed by coring. Cores remained open to the tank water until 30 min before sampling, when clear Plexiglas lids were fitted to each core liner to seal in overlying water within the core for the duration of the incubation (~15 h). Dissolved oxygen (± 0.01 mg L^{-1}) and pH (± 0.002 pH) were measured optically and electrically (Hach HQ40d multi-parameter meter) via a sampling port in the lid. Initial samples were taken 30 min after closure of the lids, dark samples were taken after ~12 hours incubation with no light, and light samples were taken after 3 hours of illumination following the end of the dark period. Light incubations were of shorter duration to prevent supersaturation of dissolved oxygen which would have

compromised additional analyses required for a complementary study. During sampling, 50 ml of water was syringe-filtered (precombusted GF/F) into precombusted 40 ml glass vials with Teflon coated septa, killed with $HgCl_2$ (20 µL saturated solution), and refrigerated prior to analysis for concentration and $\delta^{13}C$ of DIC and DOC. Sample water was simultaneously replaced by water held in replacement bags as sampling occurred at each time point. No samples were collected for analysis of gaseous CO_2 fluxes from exposed sediments, as this was previously determined to be a negligible pathway for loss of MPB-C at this site (Oakes and Eyre 2014). At the end of sampling for the light period, cores were extruded, sectioned and sampled for Chl-α in the same manner as control cores and stored frozen (-20°C). Eight cores (two cores per treatment) were sampled in this manner for water column fluxes, PLFAs, and sediment OC after 1.5 d, 2.5 d and 3.5 d of incubation. These sampling time periods were chosen to capture the active dynamics of ^{13}C processing that were expected to occur over the first few days of the study, based on previous work by Oakes and Eyre (2014). Additionally, 8 cores (two cores per treatment) were sampled for only PLFAs and sediment OC at 0.5 d of incubation.

2.7 Sample analysis

Chl-*α* was measured by colorimetry (Lorenzen 1967) for each core (0-1 cm depth). MPB-C biomass was calculated assuming a C:Chl-*α* ratio of 40, within the range reported for algae in Australian subtropical estuaries (30-60 Ferguson et al. 2004; Oakes et al. 2012). Biomass measurements utilizing Chl-α were used to compare biomass across controls and treatments and were not utilized in calculations for uptake of ^{13}C into MPB or bacteria using PLFAs. Bacterial C biomass for controls was estimated based on MPB-C biomass derived

from Chl-α and the ratio of MPB to bacterial biomass obtained from PLFA analysis of the control cores (n=3).

Sediment samples were lyophilized, loaded into silver capsules, acidified (10% HCl), dried (60°C to constant weight), and analyzed for %C and $\delta^{13}C$ using a Thermo Flash Elemental Analyzer coupled to a Delta V IRMS via a Thermo ConFlo IV. Samples were run alongside glucose standards that are calibrated against international standards (NBS 19 and IAEA ch6). Precision for $\delta^{13}C$ was 0.1‰ with decreasing precision for enrichments above 100‰.

PLFAs specific to bacteria (i + a 15:0) were used as biomarkers for this group. However, although visual analysis confirmed the presence of a large number of pennate diatoms at the study site and diatom-specific PLFAs (e.g. 20:5(n-3)) were detected, chromatographic peaks for these PLFAs were sometimes indistinct. The 16:1(n-7) PLFA, which represents 27.4% of total diatom PLFAs (Volkman et al. 1989), was consistently present across all samples and was used as a biomarker for diatoms, following correction for contributions from gram-negative bacteria, cyanobacteria, and sulfate reducing bacteria, determined using 18:1n7 as described in the calculations section below and in Oakes et al. (2016). Extraction of PLFAs used 40 g of freeze-dried sediment and a modified Bligh and Dyer technique. Sediment was spiked with an internal standard (500 µL of 1 mg ml^{-1} tridecanoic acid, C_{13}), immersed in 30-40 ml of a 3:6:1 mixture of dichloromethane (DCM), methanol, and Milli-Q water, sonicated (15 min), and centrifuged (15 min, 9 *g*). The supernatant was removed into a separating funnel and the pellet was re-suspended in 30-40 ml of the DCM:MeOH:Milli-Q mixture, sonicated, and centrifuged twice more to ensure complete removal of biomarkers. DCM (30 ml) and water (30 ml) were added to the

239 supernatant, gently mixed, and phases were allowed to separate prior to removal of the bottom
240 layer into a round bottom flask. The top layer was then rinsed with 15 ml of DCM, gently
241 shaken, and phases allowed to separate prior to addition to the round bottom flask. This
242 extract was then concentrated under vacuum and separated using silica solid phase extraction
243 columns (Grace; 500 mg, 6.0 ml) by elution with 5 ml each of chloroform, acetone, and
244 methanol. The fraction containing methanol was retained, reduced to dryness under N_2,
245 methylated (3 ml 10:1:1 MeOH:HCl:$CHCl_3$, 80˚C, 2 h), quenched using first 3 ml and then 2
246 ml of 4:1 hexane:DCM, evaporated to ~ 200 µl under N_2, transferred to a GC vial for analysis,
247 and stored frozen (-20˚C). PLFA concentrations and $\delta^{13}C$ values were measured using a non-
248 polar 60 m HP5-MS column in a Trace GC coupled to a Delta V IRMS with a Thermo Conflo
249 III interface following the protocol outlined in Oakes et al. (2010a).

250 DIC and DOC concentrations and $\delta^{13}C$ values were measured via continuous-flow wet
251 oxidation isotope-ratio mass spectrometry using an Aurora 1030W total organic C analyzer
252 coupled to a Thermo Delta V isotope ratio mass spectrometer (IRMS) (Oakes et al. 2010b).
253 Sodium bicarbonate (DIC) and glucose (DOC) of known isotopic composition dissolved in
254 He-purged Milli-Q were used to correct for drift and verify both concentration and $\delta^{13}C$ of
255 samples. Reproducibility was ± 0.2 mg L^{-1} and ± 0.1 ‰ for DIC and ± 0.2 mg L^{-1} and ± 0.4 ‰
256 for DOC.

257 **2.8 Calculations**

258 Incorporation of ^{13}C into sediment OC, bacteria, and MPB (mmol ^{13}C m^{-2}) was
259 calculated as the product of excess ^{13}C (fraction ^{13}C in sample – fraction ^{13}C in control) and
260 the mass of OC within each pool. For sediment, OC was the product of %C and dry mass per

unit area. Percentages calculated from these pools are presented as portions of the sum of total ^{13}C contained within the sediment and the interpolated fluxes of DIC and DOC that were estimated to have occurred from 0 d until each sampling time.

Excess ^{13}C for PLFAs was determined only for 0-2 cm, 2-5 cm, and 5-10 cm depths, as there was inadequate sample mass for the 0-0.2 cm top scrape. Due to limitations of time and cost, PLFA samples were taken from only one of the two cores incubated for each treatment at each sampling period. PLFA excess ^{13}C for both bacteria and diatoms was the product of excess ^{13}C contained in the PLFA (fraction ^{13}C in PLFA in sample – fraction ^{13}C in PLFA in control) and the concentrations of C within respective biomarkers. Concentrations of PLFA C were calculated from their peak areas relative to the internal C_{13} standard spike. Biomass of diatoms and bacteria were calculated using the method described by Oakes et al. (2016). Briefly, bacterial biomass was calculated as:

1. $\text{Biomass}_{\text{bacteria}} = \text{Biomass}_{\text{i+a15:0}} / (a \times b)$

where *a* represents the average concentration of PLFA (0.056 g C PLFA per g C biomass; Brinch-Iversen and King 1990) in bacteria and *b* represents the average fraction of PLFA accounted for by i+a15:0 within bacteria-dominated marine sediments (0.16, Osaka Bay, Japan; Rajendran et al. 1994; Rajendran et al. 1993). Biomass estimates for bacteria calculated using the minimum and maximum fraction values (16-19% for i+a15:0; Rajendron et al. 1993) resulted in a 16% difference.

For diatoms, a mixing model was used to correct the concentration and $\delta^{13}C$ value of 16:1(n-7) for the any contribution from non-diatom sources. Due to the scarcity of cyanobacteria observed using light microscopy (1000×), low sediment D-/L- alanine ratios

283 measured previously at this site (as low as 0.0062, Riekenberg et al. 2017), and lack of the
284 characteristic 18:2(n-6) peak (Bellinger et al. 2009) cyanobacteria were assumed to make a
285 negligible contribution to the 16:1(n-7) peak. A two-source mixing model was applied to
286 correct the concentration and $\delta^{13}C$ value of the 16:1(n-7) peak for the contribution of gram-
287 negative bacteria, based on a typical ratio of 18:1(n-7) to 16:1(n-7) for gram-negative bacteria
288 of 0.7 (Edlund et al. 1985) as previously applied in Oakes et al. (2016). Biomass for diatoms
289 was calculated using the formula:

290 2. $\text{Biomass}_{\text{Diatom}} = \text{Biomass}_{\text{corrected16:1(n-7)}} / (c \times d)$

291 where c is the average fraction of diatom PLFAs accounted for by corrected 16:1(n-7)
292 (0.67; Volkman et al. 1989) and d is the average PLFA concentration in diatoms (0.035 g
293 PLFA C per g of C biomass; Middelburg et al. 2000). Biomass estimates for diatoms
294 calculated using maximum and minimum fraction values for 16:1(n-7) (18-33%; Volkman et
295 al. 1989) were within 50% of estimates based on the average value. Microbial biomass is the
296 sum of calculated diatom and bacterial biomass. Uncharacterized ^{13}C was calculated as:

297 3. $^{13}C_{\text{uncharacterized}} = {}^{13}C_{\text{sediment organic}} - {}^{13}C_{\text{microbial biomass}}$

298 where $^{13}C_{\text{sediment organic}}$ represents total ^{13}C in sediment organic carbon and $^{13}C_{\text{microbial}}$
299 $_{\text{biomass}}$ represents the ^{13}C contained in microbial biomass within the same core.

300 Fluxes across the sediment-water interface were calculated from two measured
301 concentrations, at the start and finish of each dark and light period (e.g., Oakes and Eyre
302 2014), as a function of incubation time, core water volume and sediment surface area. Dark
303 flux rates were calculated using concentration data from the dark incubation period and light

flux rates from the light incubation period. The following parameters were calculated from dark and light rates:

4. Respiration (R) = Dark DO flux h^{-1}
5. Net primary production (NPP) = Light DO flux h^{-1}
6. Gross primary production (GPP) = NPP + R
7. Production/respiration (P/R) = GPP x daylight hours (12 h) / R x 24 h (Eyre et al. 2011)

To prevent the potential development of resource limitations during incubation, O_2 concentrations were not allowed to drop below 60% saturation in the dark and light incubations were shortened (~3 h) to ensure that production was not allowed to become supersaturated.

Total ^{13}C in DIC and DOC (µmol ^{13}C) in the overlying water in the sediment core was calculated for initial, the end of the dark period, and the end of the light period as the product of excess ^{13}C (excess ^{13}C in labeled sample versus relevant natural abundance control), core volume, and concentration. Total excess flux of ^{13}C as DIC or DOC (µmol ^{13}C m^{-2} h^{-1}) was then calculated as:

8. Excess ^{13}C flux = (Excess $^{13}C_{start}$ – Excess $^{13}C_{end}$) / SA / t

where excess $^{13}C_{start}$ and excess $^{13}C_{end}$ represent excess ^{13}C of DIC or DOC at the start and end of dark and light incubation periods, SA is sediment surface area, and t is incubation period length (h). Net fluxes of excess ^{13}C (excess ^{13}C m^{-2} h^{-1}) for DIC and DOC were calculated as:

9. Net flux = ((dark flux * dark hours) + (light flux * light hours))/ 24 hours

Total ^{13}C lost via flux to the water column from initial labeling to each sampling period was interpolated from measured net flux values by calculating the area underneath the curve for each treatment. Because all ^{13}C was contained within the cores, values for ^{13}C budgets add to 100%. Starting values were estimated by looking at how much ^{13}C remained in the sediment and how much was lost to the water column (initial ^{13}C= ^{13}C remaining + ^{13}C lost).

2.9 Data Analysis

^{13}C remaining in sediment and MPB-C biomass was determined using chl-a data for cores within all treatments for 0.5 d, 1.5 d, 2.5 d and 3.5 d. We therefore used a two-way analysis of variance (ANOVA) to determine whether either ^{13}C remaining in sediment or MPB-C biomass were affected by treatment and/or time. P/R ratios were determined for 1.5 d, 2.5 d and 3.5 d to determine whether significant differences occurred between treatments within each time period ($\alpha = 0.05$). Levene's tests indicated that variances were homogeneous in all cases and there were no significant interactions between variables in either analysis. For significant effects of treatment or time, post hoc Tukey tests were used to identify significant differences between groups.

Total uptake for ^{13}C into both MPB and bacteria, and relative ^{13}C uptake into MPB were determined for only a single core across all treatments from 0.5 d, 1.5 d, 2.5 d and 3.5 d. To increase replication for statistical analysis, and therefore increase the power to detect a significant difference, we therefore grouped data across times into two levels: before 1.5 d (including 0.5 d and 1.5 d) and after 1.5 d (including 2.5 d and 3.5 d). There was no pooling of data across treatments. A two-way ANOVA was then used to determine whether significant differences occurred among treatments within each pooled time period ($\alpha = 0.05$). No significant interactions were observed for total uptake into MPB or bacteria, but there was a

significant interaction observed for relative ^{13}C uptake into MPB. For significant effects of interaction, treatment, time, post hoc Tukey tests were used to identify significant differences between groups.

The data for ^{13}C remaining in sediment OC were further examined by fitting an exponential decay function for each treatment across 3.5 d using the Exp2PMod1 function in OriginPro 2017 and ^{13}C turnover estimates were then determined by solving for y = 0.05 % remaining ^{13}C (a value close to 0) and x = 30 d for each treatment. Exponential decay functions were compared across treatments by dividing by 100 to convert percentages to proportions and transforming with log(n+1) to convert into linear functions with 95% confidence bands (Supplemental Fig. 2). Loss rate constants are reported as positive numbers following mathematical conventions associated with loss rates (Fig. 6).

3.0 Results

3.1 Uptake of nutrient additions

Uptake of the added nutrients into the sediment was rapid and substantial, as indicated by decreases in dissolved inorganic nitrogen ($NH_4^+ + NO_x$) concentrations in the overlying core water to $<1.2 \pm 0.1$ μM L^{-1} by 0.5 d. Across the incubation periods, elevated DIN concentrations in overlying water were occasionally observed (Supplemental Fig. 1), but corresponded with times when the cores were sealed for light and dark incubations, indicating that DIN production was a result of in-core processing rather than nutrient amendments.

3.2 Sediment characteristics

Control sediment OC content was greater in the 2-5 cm depth (187.5 ± 27.7 μmol C g^{-1}) than at all other sediment depths (112.3 ± 11.4 μmol C g^{-1} in the TS, 149.8 ± 31.6 μmol C g^{-1} at 0-2 cm, and 120.1 ± 16.5 μmol C g^{-1} at 5-10 cm). Natural abundance $\delta^{13}C$ values were most enriched in surface sediments (-18.7‰ in TS) and became progressively depleted within deeper sediments to -22.1‰ at 5-10 cm (Table 1). In the 0-2 cm depth of the control sediment, MPB-C biomass was 321.9 ± 42.0 mmol C m^{-2} and bacterial biomass was 500.4 ± 65.3 mmol C m^{-2} (Table 1).

3.3 Initial ^{13}C uptake

Uptake of ^{13}C into sediment OC occurred rapidly and was observed in the first cores collected (11 h after labeling, after tidal flushing, and with cores sectioned in the field). At this time, prior to laboratory incubation and nutrient amendment, 1549 ± 140 μmol ^{13}C m^{-2} had been incorporated into sediment OC. Sediment OC was ^{13}C-enriched across all sediment depths at this time (Table 1), but 78% of the initially incorporated ^{13}C was in the uppermost 2 cm of sediment (compared to 12.8% 2-5 cm, 9.4% 5-10 cm). Prior to incubation, ^{13}C uptake into microbial biomass at 0-2 cm was dominated by MPB (92.7 ± 1.6%), despite their lower biomass (200.2 ± 26.5 mmol C m^{-2}) compared to bacteria (311.3 ± 56.4 mmol C m^{-2}) within the labeled cores. Conversely, bacteria dominated ^{13}C uptake in 2-5 cm sediment (66.8 ± 17.2% of the ^{13}C within microbial biomass). Although sediment OC at 5-10 cm was ^{13}C-enriched, minimal uptake was detected in microbial biomarkers.

3.4 Effect of nutrient additions on P/R

Average MPB biomass remained similar across treatments over the 3.5 d incubation (two-way ANOVA: treatment $F_{3,31}$= 0.04, p=0.99; time $F_{3,31}$= 0.1, p=0.94, Supplemental Figure 3). However, there were changes in P/R ratio that varied among treatments. Examination of the effects of treatment and time on P/R showed no significant differences (two-way ANOVA: treatment $F_{3,23}$=3.0, p=0.08; time $F_{2,23}$=2.7, p=0.11), although the post hoc Tukey comparison between ambient and elevated treatments was nearly significant (p=0.0506). For the ambient, minimal and moderate treatments, P/R ratios were dominated by autotrophy and changed little over the first 2.5 d (1.5 ± 0.8, 1.2 ± 0.4, and 1.3 ± 0.1, respectively, Fig. 1b) as any increases in production were offset by increased respiration (Fig. 1a). By 3.5 d the minimal treatment had shifted into heterotrophy (0.6 ± 0.1) as a result of increased respiration and decreased production., whereas P/R ratios for the ambient and moderate treatments remained essentially unchanged (1.3 ± 0.2, 1.3 ± 0.4). P/R in the elevated treatment was initially high compared to all other treatments (2.2 ± 0.2 at 0.5 d) indicating strong dominance of autotrophic production (Fig. 1a & B). However, P/R in the elevated treatment decreased to 1.1 ± 0.4 after 3.5 d (Fig. 1), indicating a strong shift away from autotrophy and towards dominance of heterotrophic processes as respiration increased and production decreased (Fig. 1a).

3.5 Incorporation of ^{13}C into sediment organic carbon

3.5.1 Uptake of ^{13}C into 0-2 cm sediment

At 0.5 d, the ^{13}C incorporated into sediment OC was predominantly contained in the 0-2 cm depth across all treatments (~65%-90%, Fig. 2) and was statistically similar across treatments (one-way ANOVA: $F_{3,7}$= 4.2, p=0.1). By 3.5 d, ^{13}C retention was lower within sediment from nutrient amended treatments compared to the ambient treatment. Whereas the

411 ^{13}C contained in the 0-2 cm depth in the ambient treatment was similar across 3.5 d (78.9 ±
412 8.8% 1.5 d, 77.0 ± 16.4% 2.5 d, 81.6 ± 4.4% 3.5 d), the ^{13}C content decreased in the minimal,
413 moderate and elevated treatments to 70.3 ± 8.3%, 73.6 ± 16.4%, and 68.8 ± 7.6%, respectively
414 (Fig. 2).

415 **3.5.2 Downward transport below 2 cm**

416 Downward transport of newly labeled material to 2-5 cm depth was low across all
417 treatments, but was higher for the elevated treatment at both 0.5 and 2.5 d. At 0.5 d there was
418 less downward transport in minimal and moderate treatments compared to the ambient and
419 elevated treatments. By 2.5 d downward transport was similar for ambient, minimal and
420 moderate treatments (10%, 9%, 10%, respectively; Fig. 2), but was considerably higher in the
421 elevated treatment (28.4%). By 3.5 d, ^{13}C incorporation into 2-5 cm sediment OC was
422 similarly low for ambient, minimal and moderate treatments (8.0 ± 2.1%, 11.1 ± 0.1%, and 8.7
423 ± 2.1%, respectively), but lower in the elevated treatment (4.8 ± 2.1%). At 0.5 d, downward
424 transport into the 5-10 cm layer was a relatively small portion of initial ^{13}C, but was higher in
425 ambient and minimal treatments (8.7 ± 2.4% and 11.6 ± 1.5%) when compared to moderate
426 and elevated treatments (2.3 ± 1.9% and 6.8 ± 0.1%, Fig. 2). Downward transport below 5 cm
427 was similar (5-11%) for all treatments at 2.5 d and 3.5 d.

428 **3.6 ^{13}C distribution amongst sediment compartments**

429 **3.6.1 Microbial biomass**

430 The total ^{13}C content of MPB (mmol ^{13}C m^{-2}; Fig. 4a) decreased significantly from
431 before 1.5 d to after 1.5 d for all treatments (two-way ANOVA: $F_{1,8}$=12.2, p=0.008), but there
432 was no significant difference among treatments (two-way ANOVA: $F_{3,8}$=2.7, p=0.12). The
433 total ^{13}C content of bacteria (mmol ^{13}C m^{-2}; Fig. 4a) did not change significantly with time,

434 and was not significantly affected by treatment. The majority of the ^{13}C assimilated into the
435 cores was present in the 0-2 cm depth (0-2 cm 2-5 cm 9 ± 0.8%; and 5-10 cm 5.2 ± 0.5%
436 Supplemental Fig. 4a, b & c). ^{13}C incorporation was largely dominated by bacteria across all
437 treatments in sediments below 2 cm, with few exceptions. Increased bacterial contribution
438 occurred more quickly and was more pronounced in nutrient amended treatments at both 2-5
439 cm and 5-10 cm (Supplemental Figs. 5 & 6).

440 Total uptake of excess ^{13}C (Fig. 4a), while informative about the amount of label
441 contained within each core at each time period, is not as useful for comparison between
442 microbial groups due to variations in the total amount of ^{13}C assimilated between cores. It is
443 important to consider the relative contribution to ^{13}C uptake (Fig. 4b) of both microbial groups
444 as each data point was sampled from separate cores that assimilated similar, but different,
445 initial concentrations of newly fixed ^{13}C. Significant MPB contribution (%) decreased for after
446 1.5 d (two-way ANOVA: $F_{1,8}$= 83.1, p<0.0001) but showed no difference between treatments
447 ($F_{3,8}$=8.2, p=0.008), although interaction between the variables was significant ($F_{3,8}$=8.2,
448 p=0.008). Tukey tests found that MPB contributed less to microbial uptake of ^{13}C in the
449 elevated treatment than in the ambient treatment (p=0.01) as well as the moderate treatment
450 being lower than the minimal treatment (p=0.014). MPB dominated the relative incorporation
451 of ^{13}C into microbial biomass at 0-2 cm in all treatments initially (0.5d; 90% ambient, 90%
452 minimal, 92% moderate, and 92% elevated; Fig. 4b) and throughout the 3.5 d incubation (81-
453 90% ambient, 82-91% minimal, 74-92% moderate, and 65-92% elevated; Fig. 4b). The
454 relative bacterial contribution to microbial ^{13}C incorporation increased across all treatments as
455 the incubations progressed, but increases in the moderate and elevated treatments at 2.5 and
456 3.5 d (Fig. 4b) corresponded with decreased ^{13}C incorporation into MPB (Fig. 4a).

3.6.2 Uncharacterized

A portion of the ^{13}C contained within sediment OC was uncharacterized, i.e., not contained within the viable microbial biomass measured using PLFA biomarkers. Initially (0.5 d) the uncharacterized pool accounted for less sediment ^{13}C within the nutrient-amended treatments (1-3%) than within the ambient treatment (12%; Fig. 3), indicating that there was more ^{13}C contained in viable microbial biomass under increased nutrient availability after 12 h of incubation. By 3.5 d increased contribution to the uncharacterized pool in the moderate and elevated treatments (29% ambient, 32% minimal, 41% moderate and 45% elevated; Fig. 3) corresponded with decreased ^{13}C contained in MPB (52% ambient, 49% minimal, 42% moderate and 26% elevated). In contrast, changes in the ^{13}C in the uncharacterized pool did not relate to ^{13}C contained in bacteria, as the bacterial contribution to ^{13}C remained relatively unchanged (17% ambient, 14% minimal, 15% moderate and 15% elevated) and was similar among treatments at 3.5 d.

3.7 Loss of ^{13}C from sediment OC

The total ^{13}C remaining in sediment (Fig. 6) varied significantly among treatments (two-way ANOVA: $F_{3, 31}= 5.7$, $p=0.008$) and across sampling times ($F_{3, 31}= 3.9$, $p=0.03$). Throughout the study, there was generally less ^{13}C remaining within the elevated treatment than in than either the ambient ($p=0.008$) or minimal treatments ($p=0.02$), and there was significantly less ^{13}C remaining within the sediment at 3.5 d than at 0.5 d ($p=0.02$). Rates of ^{13}C loss from sediment OC to the water column were highest in the moderate and elevated treatments (total lost at 3.5 d: ambient 5%, minimal, 7%, moderate 11% and elevated 20%; Fig. 5 & 6). Reflecting this, loss rate constants for the ^{13}C remaining in sediment OC after accounting for losses of $DI^{13}C$ and $DO^{13}C$ across 3.5 d were equivalent for ambient and

480 minimal treatments (0.018 ± 0.024, R^2 = 0.95 and 0.021 ± 0.001, R^2 = 0.99, respectively; Fig.
481 6), but were higher for both moderate and elevated treatments (0.0383 ± 0.009, R^2 = 0.86,
482 0.0566 ± 0.003, R^2 = 0.99, respectively; Fig. 6). Since the intercept is known, i.e., the initial
483 value equals 100% at time 0, linear models where only the slopes were estimable, were fitted
484 to further analyze the differences between slopes. Assuming an exponential decay, the
485 percentage remaining ^{13}C (Y) was $\log_{10}$ transformed and the value 2 was subsequently
486 subtracted ($Z=\log_{10}(Y) -2$), which implies that the intercept of Z versus time equals 0. The
487 model with different slopes for each treatment fitted significantly better than the model with a
488 single slope (F-test, $F_{3,28}$=9.84, P <0.001, Supplemental Fig. 2). The analysis was performed
489 in R.

490 Across all treatments, most of the ^{13}C loss from sediment during the incubation
491 occurred via DIC fluxes (Fig. 5). Cumulative ^{13}C export to the water column via DIC fluxes
492 was considerably larger than via DOC fluxes for all treatments (9× ambient, 11× minimal, 10×
493 moderate and 17× elevated). Initial $DI^{13}C$ loss (0.5 d) was higher in the elevated treatment
494 than in the ambient, minimal, and moderate treatments (5.3 ± 3.4%, versus 0%, 1.1 ± 0.3%
495 and 1.4 ± 1.4%, respectively; Fig. 5). After 3.5 d, cumulative losses of $DI^{13}C$ were higher in
496 moderate and elevated treatments (12.4 ± 11.6% moderate, 19.8 ± 10.8% elevated; Fig. 5)
497 than in ambient (4.0 ± 3.2%) and minimal treatments (6.6 ± 2.0%; Fig. 5 & 7).

498 DOC export was a less important pathway for ^{13}C loss than DIC across all treatments.
499 ^{13}C loss via DOC export was comparable and low across all treatments with similar maximum
500 export at 3.5 d (0.5 ± 0.2% ambient, 0.5 ± 0.2% minimal, 0.4 ± 0.2% moderate, and 0.6 ±
501 0.5% elevated; Fig. 5).

4.0 Discussion

This study examined the effects of enhanced nutrient loading on the processing pathways for MPB-derived C in intertidal estuarine sediments. Enhanced nutrient availability 1) increased loss of MPB-derived C from sediment via DIC efflux (Fig. 5 & 6), 2) shifted benthic metabolism to be less autotrophic (Fig. 1), and 3) decreased retention of C within MPB (Fig. 3 & 4). These multiple lines of evidence indicate that intertidal sediments in areas experiencing increased nutrient loading are likely to process C differently, resulting in reduced potential for C retention within the sediment.

4.1 Loss pathways for ^{13}C

Increased nutrient additions caused additional loss of ^{13}C from sediment OC, largely driven by DIC fluxes to the water column (Fig. 5 & 6). Complete loss of newly produced C from sediment OC, as estimated from exponential decay functions, occurred more quickly in nutrient amended treatments than in ambient (15% increase minimal, 210% increase moderate and 310% increase elevated, Fig. 6). Increased loss rates indicated reduced turnover time for newly produced MPB-derived C under increased nutrient load (419 d ambient versus 199 d moderate and 134 d elevated). It should be noted that the loss rate constant for the minimal treatment (0.021 ± 0.001, $R^2 = 0.99$, 366 d) was comparable to that for the ambient treatment (0.018 ± 0.024, $R^2 = 0.95$, 419 d), indicating that a small nutrient addition may not cause significant decreases in C turnover time. Increased loss rates imply that C retention and burial in MPB-dominated photic sediments are greatest when nutrients are limiting and that increased nutrient availability alters the processing of MPB-C within the sediment. Increased nitrogen availability appears to have decreased the retention of C within MPB biomass (Fig. 3). Increased turnover of the newly fixed MPB-derived C from the sediment likely occurred as

525 the net result of exudation of material and breakdown of cells. This increased turnover may
526 have caused the increased efflux of MPB-derived C as exudates and cell components were
527 increasingly available to support respiration. The focus of this study was short-term fate of
528 MPB-C, but our findings also show potential implications for longer- term retention. Our
529 calculated retention times may be under or over-estimated due to their reliance on short-term
530 data. However, the relative differences between treatments (decreased retention with increased
531 nutrient amendment) are clear. The rationale for utilizing exponential functions in this study
532 follows previous findings in Oakes et al. (2014) that ^{13}C export from subtidal sediments at this
533 site were well-described by an exponential decay function across a longer time period (31 d).
534 Additionally, the 30 d estimates provided within this study (18-58%) fall across a range
535 similar to that of other previous labeling experiments (30-50%; Hardison et al. 2011; Oakes
536 and Eyre 2014; Oakes et al. 2012), leading the authors to conclude that the use of exponential
537 functions to describe this relationship was valid in this study.

538 Across all treatments, DIC was the main loss pathway for MPB-C, DOC was a minor
539 pathway and loss via CO_2 was considered negligible (Oakes and Eyre 2014) (Fig. 5 & 6). Loss
540 of ^{13}C via the DIC pathway appears to be stimulated by nutrient additions, resulting in
541 increased export occurring earlier within incubations as a result of increased bacterial
542 remineralization (Fig. 2 & 5). Increased $DI^{13}C$ export represents the portion of $DI^{13}C$
543 produced via respiration in excess of that which is re-captured and utilized by MPB to drive
544 production. Given the close proximity of bacteria and MPB in the sediment, there is the
545 potential for considerable utilization of the $DI^{13}C$ arising from bacterial remineralization to
546 support algal production. Relatively low fluxes of $DI^{13}C$ to the water column in the ambient
547 treatment across 2.5 d likely indicate more complete utilization and recycling of $DI^{13}C$ to

548 support algal production (Fig. 5). Export of $DI^{13}C$ was considerably higher in both the
549 moderate and elevated treatments, indicating production of $DI^{13}C$ during bacterial
550 remineralization in excess of utilization of $DI^{13}C$ by MPB. Decreased recycling of $DI^{13}C$ from
551 remineralization in elevated treatments could develop due to 1) decreased DIC demand as
552 algal production decreased after initial stimulation or 2) increased production of unlabeled
553 DIC through remineralization of previously refractory organic material providing an
554 alternative unlabeled source to support algal production.

555 Cumulative losses of $DO^{13}C$ were low for all treatments across 3.5 d (<1.5 % of total
556 ^{13}C, Fig.5) and did not appear to change significantly with increased nutrient availability.
557 Previous studies have also found that DOC fluxes are a relatively minor contributor to loss of
558 MPB-derived carbon (Oakes et al. 2012; Oakes and Eyre 2014), as observed in the current
559 study, but DOC may be a significant export pathway in other settings. Produced DOC may be
560 labile and respired to DIC prior to loss from the sediment, but this pathway was not greatly
561 altered in this study due to increased nutrient availability.

562 **4.2 Shifts in benthic metabolism**

563 Each nutrient amendment produced a different shift in benthic metabolism within the
564 core incubations (Fig. 1) with no clear dose-effect relationship between increased nutrient
565 availability and P/R observed among nutrient-amended treatments. Heterogeneity in both
566 bacterial and MPB biomass are routinely observed within intertidal sediment and can lead to
567 substantial variability between the production and respiration observed between cores (Eyre et
568 al. 2005; Glud 2008). Despite a background of variability between cores, both minimal and
569 elevated treatments display a decrease in autotrophy. The minimal treatment shifted into
570 heterotrophy (P/R<1) and the elevated treatment stimulated initial algal production sufficient

to cause a subsequent spike in respiration. Increased respiration by 3.5 d was partially offset by maintained production that kept P/R above 1. In contrast, the moderate treatment maintained a steady P/R across 3.5 d, although substantial error bars indicate considerable variability between the cores within the treatment. MPB-dominated sediment is expected to be net autotrophic, with positive GPP (Tang and Kristensen 2007) that may be further stimulated by nutrient inputs (Underwood and Kromkamp 1999). Increased algal production of labile organic matter subsequently stimulates heterotrophic respiration, increasing oxygen consumption and lowering P/R (Glud 2008; McGlathery et al. 2007). Quick increases in MPB productivity followed by increased respiration have been observed in response to pulses of organic matter in both oligotrophic and estuarine sediments (Eyre and Ferguson 2005; Glud et al. 2008). Rapid increases in respiration rates, as reflected in the oxygen fluxes for the elevated treatment (Fig. 1a), are often associated with an increased supply of labile C and can occur at rates higher than expected for in situ temperature. This has been observed in subtropical sediments (Eyre and Ferguson 2005) as well as polar and temperate systems (Banta et al. 1995; Rysgaard et al. 1998). Although the sediments in this study were not oligotrophic, the extent of the shift towards heterotrophy is still likely controlled by the amount and relative quality (C/N ratio) of the organic matter available for processing (Cook et al. 2009; Eyre et al. 2008). It is important to note that the elevated treatment did not shift to a P/R less than 1, but did display a considerable increase in respiration. The rapid increase in respiration in the elevated treatment suggests that the newly produced organic matter was readily bioavailable and quickly processed by bacteria as a result of increased nutrient availability.

4.3 Retention of carbon within microphytobenthos biomass

Within surface sediments, MPB biomass did not increase with increased nutrient load, despite apparent increases in productivity (Supplemental Fig. 3). Although MPB biomass did not change, by 3.5 d the ^{13}C retained within MPB biomass in the nutrient-amended treatments appears to have decreased (Fig. 4a) indicating increased turnover of newly fixed C out of MPB biomass. This aligns with many previous reports that increased productivity does not necessarily correspond with increased algal biomass (Alsterberg et al. 2012; Ferguson and Eyre 2013; Ferguson et al. 2007; Hillebrand and Kahlert 2002; Piehler et al. 2010; Spivak and Ossolinski 2016). Lack of change in MPB biomass, despite increased productivity, may occur as a result of grazing or secondary nutrient limitation (Hillebrand and Kahlert 2002), but these explanations are unlikely for the current study. Grazing is likely to have occurred at only a low level. There was very little fauna, including grazers, within sediment at the study site and, although any grazers such as copepods that were within the site water would have been included in the incubations, larger, mobile grazers were excluded. Secondary nutrient limitation of P or Si was avoided through additions of both elements at 0 d for P and 2.5 d for Si during incubation. It is more likely that the microbial community responded to pulses of increased nutrients through increased production of extracellular compounds (MPB: carbohydrates; bacteria: enzymes) rather than increasing their biomass (Thornton et al. 2010). This may be a strategy to optimally utilize intermittently available nutrient resources, given that increased cell numbers (biomass) within a biofilm community may otherwise increase competition among cells (Decho 2000; Drescher et al. 2014). Allocation of additional N towards increased production of extracellular enzymes or storage molecules rather than new biomass may therefore benefit the community. Strong competition between MPB and bacteria

for available N resulted in a minimal contribution from denitrification as a pathway for N loss likely as a result of limited availability of NO_3^- for denitrifying bacteria (unpubl. data).

4.4 ^{13}C distribution within the sediment

4.4.1 Microbial biomass

Decreased autotrophy is somewhat reflected in the relative partitioning of ^{13}C from newly produced algal C between MPB and bacteria within the individual treatments (Fig. 1 & Fig. 4b). Initially, uptake of ^{13}C was strongly dominated by MPB amongst treatments, with minimal incorporation by bacteria. As incubations progressed, a shift towards increased relative contribution by bacteria was apparent in all treatments, but was more substantial in the elevated treatment (3.5 d; 19% ambient, 18% minimal, 26% moderate, and 35% elevated, Fig. 4b). This quicker shift towards bacterial dominance of ^{13}C incorporation corresponded with the largest decrease in P/R ratios observed in this study, as increased respiration and decreased production caused the elevated treatment to become less autotrophic (Fig. 1). These corresponding factors are likely a result of a tight coupling and intense recycling between algal production and bacterial processing of newly produced MPB-derived C. EPS can be a large export pathway for newly fixed C from algal cells (up to 70.3% Goto et al. 1999) and can provide a labile C source for heterotrophic or denitrifying bacteria. The ^{13}C incorporated into bacteria represents the balance of respiration and uptake and is expected to become increasingly muddled by ^{13}C being processed through other pathways (denitrification) as incubations progress. Therefore, this study only considered the transfer of MPB-C into bacteria at the 0.5 d sampling. However, given the low initial transfer of ^{13}C to bacteria in all treatments over 24 h following labeling (0.5 d; 0.8% h^{-1} ambient, 0.8% h^{-1} minimal, 0.7% h^{-1} moderate, 0.7% h^{-1} elevated; Fig. 3) it appears that either production or utilization of EPS

containing newly fixed C was relatively low in the current study, regardless of nutrient addition. This transfer was the net result of EPS production and bacterial remineralization and would have become increasingly muddled as ^{13}C-containing detrital material accumulated as incubations progressed. Low EPS production at 0.5 d may indicate that N is not limiting for MPB in these sediments, as exuded EPS does not appear to be copious, as would be expected under severe N limitation (van Den Meersche et al. 2004). Similarly low rates of C transfer from MPB to bacteria were previously reported for the site (0.83% h^{-1}, Oakes and Eyre 2014) and are towards the lower end of the range of EPS production rates for benthic diatoms (0.05 to 73% h^{-1}; Underwood and Paterson 2003). At 0.5 d nutrient availability appears to have had little effect on the initial transfer rates from MPB to bacteria, but appears to have decreased the turnover of MPB-C out of the microbial community, as contributions of ^{13}C to the uncharacterized pool were lower in the nutrient-amended treatments (Fig. 3). By 3.5 d, increased nutrient availability appears to stimulate the transfer of ^{13}C from microbial biomass in the uncharacterized pool, but had no effect on ^{13}C in bacteria as the bacterial pool was equal across all treatments (15-18%, Fig. 3 & 7).

4.4.2 Uncharacterized

A portion of the ^{13}C incorporated into sediment OC was uncharacterized (i.e., not within microbial biomass). By 3.5 d, the portion of initially incorporated ^{13}C that was within the uncharacterized pool varied substantially among the treatments (29-46%, Fig. 7). This uncharacterized C is likely to represent a mixture of both labile and refractory OC (Veuger et al. 2012), including metabolic byproducts, senescent cells undergoing breakdown, EPS, extracellular enzymes, carbohydrates, and a variety of complex, molecularly uncharacterized organic matter (Hedges et al. 2000). Collectively, these molecules form a pool of labeled intra

662 and extra-cellular material remaining in sediment OC derived from both MPB and bacteria
663 that is not characterized as microbial biomass when using PLFAs to estimate microbial
664 biomass (e.g., ^{13}C contained in storage products or enzymes that was not incorporated into
665 phospholipids). Given that MPB can direct up to 70% of their newly fixed C to EPS (Goto et
666 al. 1999), carbohydrates are likely to form a considerable portion of the uncharacterized ^{13}C.
667 A study using a similar ^{13}C-labeling approach reported that 15-30% of MPB-derived carbon
668 was transferred to intra- and extracellular carbohydrates within 30 d after an initial transfer
669 rate of ~0.4% into bacteria (2 d; Oakes et al. 2010a). In light of the higher transfer rates for
670 ^{13}C into bacteria observed in this study (0.7 to 0.9% h^{-1}), there is potential for a considerable
671 portion of the uncharacterized pool to be accounted for by EPS.

672 When quantified, the uncharacterized C pool typically has a high C:N ratio (10 to 60;
673 Cook et al. 2009; Eyre et al. 2016a), indicating that nitrogen availability may have a role in
674 regulating its content and accumulation. Given that nitrogen limitation has been observed to
675 suppress processing pathways of otherwise labile OM in soils (Jian et al. 2016; Schimel and
676 Bennett 2004), a similar mechanism may be possible in estuarine sediments. This mechanism
677 may include a priming effect due to either increased production of extracellular enzymes or
678 due to increased energy from labile C compounds allowing for the increased breakdown of
679 sediment OM (Bianchi 2011). Increased extracellular enzyme production would result in more
680 complete utilization of sediment OM through promotion of hydrolysis (Arnosti 2011; Huettel
681 et al. 2014), a potentially limiting step during the breakdown of organic material. This would
682 result in more complete utilization of ^{13}C by microbial biomass and a smaller pool of
683 uncharacterized C within sediment OC, as was observed in the nutrient-amended treatments at
684 0.5 d (Fig. 3). This is further supported by the increased turnover of MPB-C from microbial

biomass into the uncharacterized pool observed within the nutrient amended treatments (2.5 d, Fig. 3) indicating ^{13}C that was previously incorporated into MPB was processed into the uncharacterized pool more quickly with increased nutrient availability. After 2.5 d, the ^{13}C content of the uncharacterized pool was substantially larger for the elevated treatment (Fig. 3 & 7) and looks to have been largely sourced from MPB ^{13}C, given that bacterial contribution to sediment OM remained stable. Composition of the uncharacterized pool will be study-specific depending on the different biomarker techniques utilized to estimate microbial biomass incorporating different pools of material. The metabolic pathways and ecological strategies regulating the portion of ^{13}C entering the uncharacterized pool warrant further investigation.

4.5 Downward transport

Increased nutrient availability reduced the downward transport of fixed ^{13}C, particularly within 2-5 cm, mainly as a result of increased export of MPB-C to the water column. In the ambient treatment, downward transport to 2-5 cm (10.0%) and 5-10 cm (9.2%) across 60 h was comparable to that reported by Oakes and Eyre (2014) for the same site (8.3% 2-5 cm, 14.9% 5-10 cm, 60 h). Oakes and Eyre (2014) suggested that resuspension resulting from a flood event limited the downward transport of ^{13}C, but a comparable and lower rate of downward transport at 60 h (12.1% 2-5 cm, 9% 5-10 cm, ambient treatment) was observed in the current study in the absence of marked freshwater inflow. Downward transport is not a large pathway for loss of ^{13}C within this system as transport to sediment below 2 cm was minimal, and appeared further reduced in the elevated treatment (Supplemental Fig. 4b & c). Decreased downward transport of MPB-derived C under increased nutrient load may reflect 1) decreased transport to depth as diatoms reduce migration downward to find nutrients

708 (Saburova and Polikarpov 2003) or 2) relaxation of the tight recycling and retention of newly
709 fixed C between MPB and bacteria within surface sediments allowing for increased export of
710 labile C to the water column (Cook et al. 2007). Decreased downward transport in this study
711 likely reflects a combination of reduced algal transport of ^{13}C to depth and increased loss of
712 ^{13}C from surface sediments to the water column.

713 **4.6 Implications**

714 This study has provided valuable insight into the processing of MPB-derived C under
715 increased nutrient availability using multiple lines of evidence (budgeting ^{13}C within sediment
716 compartments and sediment-water effluxes, partitioning of C pools via biomarkers, and
717 changes in P/R) and is among the first to have addressed this problem. However, some caveats
718 on interpretation are important to note, as follows: 1) *Ex situ* incubation of sediment cores
719 may not be directly comparable to processes occurring *in situ* and may overestimate C
720 retention, as there is reduced potential for loss via sediment resuspension due to tidal
721 movement, water currents, and grazing. 2) Removal of grazers may also increase MPB
722 production and their release of exudates (Fouilland et al. 2014), which could enhance ^{13}C
723 transfer to bacteria. However, given the lack of apparent grazers at the site of the current
724 study, and the low observed ^{13}C transfer rate to bacteria (0.7-0.9% h^{-1} Fig. 4b) that was
725 comparable to previously measured in situ rates in Oakes and Eyre (2014), grazers appear to
726 have had little potential impact on sediment processing in this study.

727 The findings show that increased nutrient availability reduced C retention, but the
728 main export pathway for algal carbon remained the same (primarily loss via DIC). Coastal
729 environments are recognized as important sites for carbon storage. Although the focus has
730 primarily been on vegetated environments (Duarte et al. 2005), which store the most carbon,

731 unvegetated sediments also have capacity for longer-term retention (e.g. ~50% after 21 d
732 Hardison et al. 2011, 30% after 30 d Oakes and Eyre 2014; 31% after 30 d Oakes et al. 2012).
733 Based on N burial rates (and corresponding unpublished C burial rates) some coastal systems
734 can have higher C burial rates in subtidal and intertidal macrophyte-free MPB sediments than
735 in macrophyte-dominated sediments (Eyre et al. 2016b; Maher and Eyre 2011) although this
736 was shown in only one of the three estuaries studied. Increased nutrient loading into coastal
737 settings has been implicated in historical decreases of long-term carbon storage through a shift
738 from macrophyte dominated systems (seagrass and mangrove) towards MPB dominated
739 systems (Macreadie et al. 2012) within coastal environments. Carbon storage potential within
740 MPB dominated sediments remains a significant knowledge gap within the carbon budgets of
741 estuaries. The primary focus of this study was short-term fate of MPB-C, but the significant
742 decrease in retention observed with nutrient amendments imply that short-term processes may
743 have implications for longer term retention. It is interesting to consider how these short-term
744 changes may affect the longer-term retention (30 d) reported by previous studies (e.g., Oakes
745 & Eyre 2014), with the caveat that the substantial extrapolation required could introduce
746 considerable error to estimates of retention. At 30 d, estimates of retention of C identified for
747 ambient and minimal treatments were considerable in the current study (58% and 54%),
748 however, increased nutrient loading reduced this retention considerably (32% moderate, 18%
749 elevated). Given that nutrient inputs have increased globally and bare photic sediment
750 accounts for a large surface area within estuaries, these two factors could have resulted in
751 substantial release of currently stored carbon and demonstrate the capacity for further
752 substantial reduction of C storage potential globally if elevated nutrient inputs continue within
753 estuarine systems.

Although MPB-dominated sediments probably have less decadal-scale long-term storage of C than macrophyte-dominated sediments, this study clearly demonstrates that the existing storage potential is further degraded by increased nutrient loading within MPB-dominated sediments. These sediments may lock away less C per area, but are fairly ubiquitous within photic coastal and oceanic sediment and may contribute significantly to carbon storage within coastal systems due to this increased area. The observed increases in mobility of newly fixed algal carbon from intertidal sediments (Fig. 5) as a result of elevated anthropogenic nutrient loading will directly translate to increased carbon export to coastal oceans and reduced carbon storage potential within shallow photic estuarine sediments.

References

Alsterberg, C., K. Sundback, and S. Hulth. 2012. Functioning of a shallow-water sediment system during experimental warming and nutrient enrichment. Plos One **7:** 10.

Andersson, J. H. and others 2008. Short-term fate of phytodetritus in sediments across the Arabian Sea Oxygen Minimum Zone. Biogeosciences **5:** 43-53.

Armitage, A. R., and P. Fong. 2004. Upward cascading effects of nutrients: shifts in a benthic microalgal community and a negative herbivore response. Oecologia **139:** 560-567.

Arnosti, C. 2011. Microbial extracellular enzymes and the marine carbon cycle. Ann. Rev. Mar. Sci. **3:** 401-425.

Banta, G. T., A. E. Giblin, J. E. Hobbie, and J. Tucker. 1995. Benthic respiration and nitrogen release in Buzzards Bay, Massachusetts. J. Mar. Res. **53:** 107-135.

Bauer, J. E., W. J. Cai, P. A. Raymond, T. S. Bianchi, C. S. Hopkinson, and P. G. Regnier. 2013. The changing carbon cycle of the coastal ocean. Nature **504:** 61-70.

Bellinger, B. J., G. J. C. Underwood, S. E. Ziegler, and M. R. Gretz. 2009. Significance of diatom-derived polymers in carbon flow dynamics within estuarine biofilms determined through isotopic enrichment. Aquat. Microb. Ecol. **55:** 169-187.

Bianchi, T. S. 2011. The role of terrestrially derived organic carbon in the coastal ocean: A changing paradigm and the priming effect. P. Natl. Acad. Sci. **108:** 19473-19481.

781 Brinch-Iversen, J., and G. M. King. 1990. Effects of substrate concentration, growth state, and
782 oxygen availability on relationships among bacterial carbon, nitrogen and
783 phospholipid content. FEMS Microb. Ecol. **74:** 345-356.
784 Cook, P., D. Van Oevelen, K. Soetaert, and J. Middelburg. 2009. Carbon and nitrogen cycling
785 on intertidal mudflats of a temperate Australian estuary. IV. Inverse model analysis
786 and synthesis. Mar. Ecol. Prog. Ser. **394:** 35-48.
787 Cook, P. L. M., B. Veuger, S. Boer, and J. J. Middelburg. 2007. Effect of nutrient availability
788 on carbon and nitrogen and flows through benthic algae and bacteria in near-shore
789 sandy sediment. Aquat. Microb. Ecol. **49:** 165-180.
790 Decho, A. W. 2000. Microbial biofilms in intertidal systems: an overview. Cont. Shelf Res.
791 **20:** 1257-1273.
792 Drenovsky, R. E., G. N. Elliott, K. J. Graham, and K. M. Scow. 2004. Comparison of
793 phospholipid fatty acid (PLFA) and total soil fatty acid methyl esters (TSFAME) for
794 characterizing soil microbial communities. Soil Biol. Biochem. **36:** 1793-1800.
795 Drescher, K., Carey d. Nadell, Howard a. Stone, Ned s. Wingreen, and Bonnie l. Bassler.
796 2014. Solutions to the public goods dilemma in bacterial biofilms. Curr. Biol. **24:** 50-
797 55.
798 Duarte, C. M., J. J. Middelburg, and N. Caraco. 2005. Major role of marine vegetation on the
799 oceanic carbon cycle. Biogeosciences **2:** 1-8.
800 Edlund, A., P. D. Nichols, R. Roffey, and D. C. White. 1985. Extractable and
801 lipopolysaccharide fatty acid and hydroxy acid profiles from *Desulfovibrio* species. J.
802 Lipid Res. **26:** 982-988.
803 Evrard, V., M. Huettel, P. L. M. Cook, K. Soetaert, C. H. R. Heip, and J. J. Middelburg. 2012.
804 Importance of phytodetritus and microphytobenthos for heterotrophs in a shallow
805 subtidal sandy sediment. Mar. Ecol. Prog. Ser. **455:** 13-31.
806 Eyre, B. 1997. Water quality changes in an episodically flushed sub-tropical Australian
807 estuary: A 50 year perspective. Mar. Chem. **59:** 177-187.
808 Eyre, B., R. N. Glud, and N. Patten. 2008. Mass coral spawning: A natural large-scale nutrient
809 addition experiment. Limnology and Oceanography **53:** 997-1013.
810 Eyre, B., J. M. Oakes, and J. J. Middelburg. 2016a. Fate of microphytobenthos nitrogen in
811 subtropical sediments: A ^{15}N pulse-chase study. Limnol. Oceanogr. **61:** 1144-156.

Eyre, B. D. 2000. Regional evaluation of nutrient transformation and phytoplankton growth in nine river-dominated sub-tropical east Australian estuaries. Mar. Ecol. Progr. Ser. **205:** 61-83.

Eyre, B. D., and A. J. P. Ferguson. 2005. Benthic Metabolism and Nitrogen Cycling in a Subtropical East Australian Estuary (Brunswick): Temporal Variability and Controlling Factors. Limnol. Oceanogr. **50:** 81-96.

Eyre, B. D., A. J. P. Ferguson, A. Webb, D. Maher, and J. M. Oakes. 2011. Metabolism of different benthic habitats and their contribution to the carbon budget of a shallow oligotrophic sub-tropical coastal system (southern Moreton Bay, Australia). Biogeochemistry **102:** 87-110.

Eyre, B. D., D. T. Maher, and C. Sanders. 2016b. The contribution of denitrification and burial to the nitrogen budgets of three geomorphically distinct Australian estuaries: Importance of seagrass habitats. Limnol. Oceanogr. **61:** 1144-1156.

Ferguson, A., and B. Eyre. 2013. Interaction of benthic microalgae and macrofauna in the control of benthic metabolism, nutrient fluxes and denitrification in a shallow sub-tropical coastal embayment (western Moreton Bay, Australia). Biogeochemistry **112:** 423-440.

Ferguson, A., B. Eyre, J. Gay, N. Emtage, and L. Brooks. 2007. Benthic metabolism and nitrogen cycling in a sub-tropical coastal embayment: spatial and seasonal variation and controlling factors. Aquat. Microb. Ecol. **48:** 175-195.

Ferguson, A., B. Eyre, and J. Gay. 2003. Organic matter and benthic metabolism in euphotic sediments along shallow sub-tropical estuaries, northern New South Wales, Australia. Aquat. Microb. Ecol. **33:** 137-154.

Ferguson, A., B. Eyre, and J. Gay. 2004. Benthic nutrient fluxes in euphotic sediments along shallow sub-tropical estuaries, northern New South Wales, Australia. Aquat. Microb. Ecol. **37:** 219-235.

Fouilland, E. and others 2014. Bacterial carbon dependence on freshly produced phytoplankton exudates under different nutrient availability and grazing pressure conditions in coastal marine waters. FEMS Microb. Ecol. **87:** 757-769.

Fry, B. and others 2015. Carbon dynamics on the Louisiana continental shelf and cross-shelf feeding of hypoxia. Estuar Coast **38:** 703-721.

Glud, R. N. 2008. Oxygen dynamics of marine sediments. Marine Biology Research **4:** 243-289.

Glud, R. N., B. D. Eyre, and N. Patten. 2008. Biogeochemical responses to mass coral spawning at the Great Barrier Reef: Effects on respiration and primary production. Limnol. Oceanogr. **53:** 1014-1024.

Goto, N., T. Kawamura, O. Mitamura, and H. Terai. 1999. Importance of extracellular organic carbon production in the total primary production by tidal-flat diatoms in comparison to phytoplankton. Mar. Ecol. Prog. Ser. **190:** 289-295.

Hardison, A., I. Anderson, E. Canuel, C. Tobias, and B. Veuger. 2011. Carbon and nitrogen dynamics in shallow photic systems: Interactions between macroalgae, microalgae, and bacteria. Limnol. Oceanogr. **56:** 1489-1503.

Hardison, A., E. Canuel, I. Anderson, C. Tobias, B. Veuger, and M. Waters. 2013. Microphytobenthos and benthic macroalgae determine sediment organic matter composition in shallow photic sediments. Biogeosciences **10:** 2791-2834.

Hedges, J. I. and others 2000. The molecularly-uncharacterized component of nonliving organic matter in natural environments. Org. Geochem. **31:** 945-958.

Hillebrand, H., and M. Kahlert. 2002. Effect of grazing and water column nutrient supply on biomass and nutrient content of sediment microalgae. Aquat. Bot. **72:** 143-159.

Huettel, M., P. Berg, and J. Kostka. 2014. Benthic Exchange and Biogeochemical Cycling in Permeable Sediments. Ann. Rev. Mar. Sci. **6:** 23-51.

Jian, S. and others 2016. Soil extracellular enzyme activities, soil carbon and nitrogen storage under nitrogen fertilization: A meta-analysis. Soil Biol. Biochem. **101:** 32-43.

Lorenzen, C. 1967. Determinations of chlorophyll and phaeopigments: spectrophotometric equations. Limnol. Oceanogr. **12:** 343-346.

Macreadie, P. I., K. Allen, B. P. Kelaher, P. J. Ralph, and C. G. Skilbeck. 2012. Paleoreconstruction of estuarine sediments reveal human-induced weakening of coastal carbon sinks. Glob. Change Biol. **18:** 891-901.

Maher, D., and B. D. Eyre. 2011. Benthic carbon metabolism in southeast Australian estuaries: Habitat importance, driving forces, and application of artificial neural network models. Mar. Ecol. Prog. Ser. **439:** 97-115.

McGlathery, K. J., K. Sundbäck, and I. C. Anderson. 2007. Eutrophication in shallow coastal bays and lagoons: The role of plants in the coastal filter. Mar. Ecol. Prog. Ser. **348:** 1-18.

McKee, L. J., B. D. Eyre, and S. Hossain. 2000. Transport and retention of nitrogen and phosphorus in the sub-tropical Richmond River estuary, Australia: A budget approach. Biogeochemistry **50:** 241-278.

Middelburg, J. J., C. Barranguet, H. T. S. Boschker, M. J. Herman, T. Moens, and C. Heip. 2000. The fate of intertidal microphytobenthos carbon: An in situ ^{13}C-labeling study. Limnol. Oceanogr. **45:** 1224-1225.

Miyatake, T., T. C. W. Moerdijk-Poortvliet, L. J. Stal, and H. T. S. Boschker. 2014. Tracing carbon flow from microphytobenthos to major bacterial groups in an intertidal marine sediment by using an in situ ^{13}C pulse-chase method. Limnol. Oceanogr. **59:** 1275-1287.

Nordström, M. C., C. A. Currin, T. S. Talley, C. R. Whitcraft, and L. A. Levin. 2014. Benthic food-web succession in a developing salt marsh. Mar. Ecol. Prog. Ser. **500:** 43-55.

Oakes, J., B. Eyre, D., J. J. Middelburg, and H. T. S. Boschker. 2010a. Composition, production, and loss of carbohydrates in subtropical shallow subtidal sandy sediments: Rapid processing and long-term retention revealed by ^{13}C-labeling. Limnol. Oceanogr. **55:** 2126-2138.

Oakes, J. M., B. Eyre, D., and J. J. Middelburg. 2012. Transformation and fate of microphytobentos carbon in subtropical shallow subtidal sands: A ^{13}C-labeling study. Limnol. Oceanogr. **57:** 1846-1856.

Oakes, J. M., and B. D. Eyre. 2014. Transformation and fate of microphytobenthos carbon in subtropical, intertidal sediments: Potential for long-term carbon retention revealed by ^{13}C-labeling. Biogeosciences **11:** 1927-1940.

Oakes, J. M., B. D. Eyre, D. J. Ross, and S. D. Turner. 2010b. Stable isotopes trace estuarine transformations of carbon and nitrogen from primary- and secondary-treated paper and pulp mill effluent. Environ. Sci. Technol. **44:** 7411-7417.

Oakes, J. M., S. Rysgaard, R. N. Glud, and B. D. Eyre. 2016. The transformation and fate of sub-Arctic microphytobenthos carbon revealed through ^{13}C-labeling. Limnol. Oceanogr. **61:** 2296-2308.

Piehler, M. F., C. A. Currin, and N. S. Hall. 2010. Estuarine intertidal sandflat benthic microalgal responses to in situ and mesocosm nitrogen additions. J. Exp. Mar. Biol. Ecol. **390:** 99-105.

Rajendran, N., O. Matsuda, Y. Urushigawa, and U. Simidu. 1994. Characterization of microbial community structure in the surface sediment of Osaka Bay, Japan, by phospholipid fatty acid analysis. Appl. Environ. Microb. **60:** 248-257.

Rajendran, N., Y. Suwa, and Y. Urushigawa. 1993. Distribution of phospholipid ester-linked fatty acid biomarkers for bacteria in the sediment of Ise Bay, Japan. Mar. Chem. **42:** 39-56.

Riekenberg, P. M., J. M. Oakes, and B. D. Eyre, 2017. Uptake of dissolved organic and inorganic nitrogen in microalgae-dominated sediment: Comparing dark and light *in situ* and *ex situ* additions of ^{15}N. Mar. Ecol. Prog. Ser. **571:** 29-42.

Rysgaard, S. and others 1998. Seasonal carbon and nutrient mineralization in a high-Arctic coastal marine sediment, Young Sound, Northeast Greenland. Mar. Ecol. Prog. Ser. **175:** 261-276.

Saburova, M. A. , and I. G. Polikarpov. 2003. Diatom activity within soft sediments: behavioural and physiological processes. Mar. Ecol. Prog. Ser. **251:** 115-126.

Schimel, J. P., and J. Bennett. 2004. Nitrogen mineralization: Challenges of a changing paradigm. Ecology **85:** 591-602.

Spivak, A. C. 2015. Benthic biogeochemical responses to changing estuary trophic state and nutrient availability: A paired field and mesocosm experiment approach. Limnol. Oceanogr. **60:** 3-21.

Spivak, A. C., and J. Ossolinski. 2016. Limited effects of nutrient enrichment on bacterial carbon sources in salt marsh tidal creek sediments. Mar. Ecol. Prog. Ser. **544:** 107-130.

Stal, L. J. 2010. Microphytobenthos as a biogeomorphological force in intertidal sediment stabilization. Ecol. Eng. **36:** 236-245.

Tang, M., and E. Kristensen. 2007. Impact of microphytobenthos and macroinfauna on temporal variation of benthic metabolism in shallow coastal sediments. J. Exp. Mar. Biol. Ecol. **349:** 99-112.

Thornton, D.C.O., S.M. Kopac, and R.A. Long. 2010. Production and enzymatic hydrolysis of carbohydrates in intertidal sediment. Aquat. Microb. Ecol. **60:** 109-125.

935 Underwood, G. J. C., and J. Kromkamp. 1999. Primary production by phytoplankton and
936 microphytobenthos in estuaries, p. 93-153. Advances in Ecological Research.
937 Underwood, G. J. C., and D. M. Paterson. 2003. The importance of extracellular carbohydrate
938 production by marine epipelic diatoms, p. 183-240. Advances in Botanical Research.
939 Academic Press.
940 Van Nugteren, P., L. Moodley, G.-J. Brummer, C. H. R. Heip, P. M. J. Herman, and J. J.
941 Middelburg. 2009. Seafloor ecosystem functioning: the importance of organic matter
942 priming. Mar. Biol. **156:** 2277-2287.
943 Van Oevelen, D., J. J. Middelburg, K. Soetaert, and L. Moodley. 2006. The fate of bacterial
944 carbon in an intertidal sediment: Modeling an in situ isotope tracer experiment.
945 Limnol. Oceanogr. **51:** 1302-1314.
946 Veuger, B., D. Van Oevelen, and J. J. Middelburg. 2012. Fate of microbial nitrogen, carbon,
947 hydrolysable amino acids, monosaccharides, and fatty acids in sediment. Geochim.
948 Cosmochim. Acta **83:** 217-233.
949 Volkman, J. K., S. W. Jeffrey, P. D. Nichols, G. I. Rogers, and C. D. Garland. 1989. Fatty acid
950 and lipid composition of 10 species of microalgae used in mariculture. J. Exp. Mar.
951 Biol. Ecol. **128:** 219-240.

952 **Author Contribution**

953 PR planned the experimental design and field work, performed the field work, isolation of
954 biomarkers and laboratory analysis, and wrote the manuscript. JO planned the experimental
955 design and field work, contributed to the data interpretation and assisted with statistical
956 analysis and writing of the manuscript. BE planned the experimental design and field work,
957 contributed to the data interpretation and assisted with the writing of the manuscript. The
958 group of co-authors has approved the submission of this manuscript.

959 **Acknowledgements**

We thank Jaap van der Meer for assistance with statistical analyses, Natasha Carlson-Perret and Jessica Riekenberg for field assistance, Iain Alexander for laboratory analysis, and Matheus Carvalho for isotope analysis. This study was funded by an Australian Research Council (ARC) Linkage Infrastructure, Equipment and Facilities grant to B.D.E. (LE0668495), an ARC Discovery Early Career Researcher Award to J.M.O. (DE120101290), an ARC Discovery grant to B.D.E. (DP160100248), and ARC Linkage Grants to B.D.E. (LP110200975; LP150100451; LP150100519).

968 **Figures and Tables**

		Top Scrape				0 to 2 cm				2 to 5 cm				5 to 10 cm			
		Biomass	SE	$\delta^{13}C$	SE	Biomass	SE	$\delta^{13}C$	SE	Biomass	SE	$\delta^{13}C$	SE	Biomass	SE	$\delta^{13}C$	SE
Control cores	Sediment organic carbon	318.0	32.3	-18.7	0.3	3818.0	804.2	-20.7	0.3	7963.3	1174.9	-22.0	0.4	8498.2	1165.2	-22.1	0.4
	Microphytobenthos biomass					321.9	42.0			226.2	33.1			227.3	37.3		
	Bacterial biomass					500.4	65.3			286.0	68.8			244.1	66.1		
Initial cores	Sediment organic carbon	376.4	4.5	121.4	23.7	3693.6	382.4	-7.5	2.1	5056.8	117.8	-19.4	1.0	8397.0	492.5	-21.4	0.7

969

970 **Table 1:** $\delta^{13}C$ values (‰) and carbon biomass (µmol C m^{-2}) for control (natural abundance,
971 n=3) and initially labeled cores (n=3, 0 d). Microphytobenthos and bacterial biomass are only
972 provided for control cores.

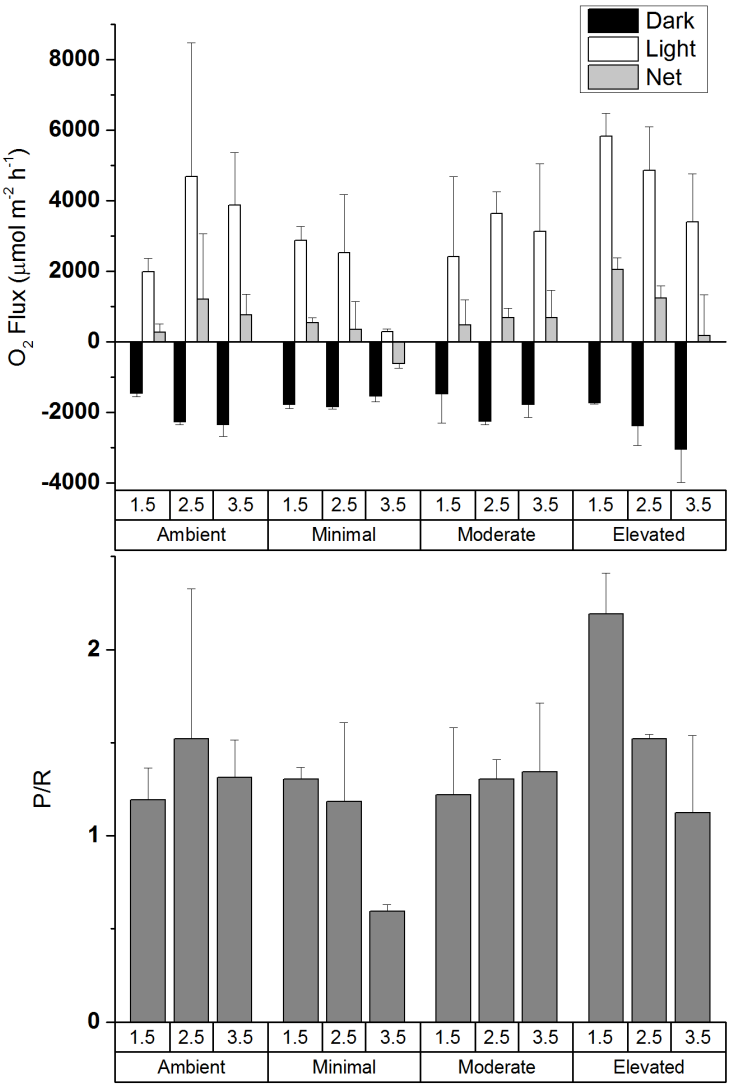

973

974 **Figure 1:** Oxygen fluxes and ratio of production to respiration (P/R) for all treatments across

975 24 h calculated from oxygen fluxes for individual cores. Values are mean ± SE.

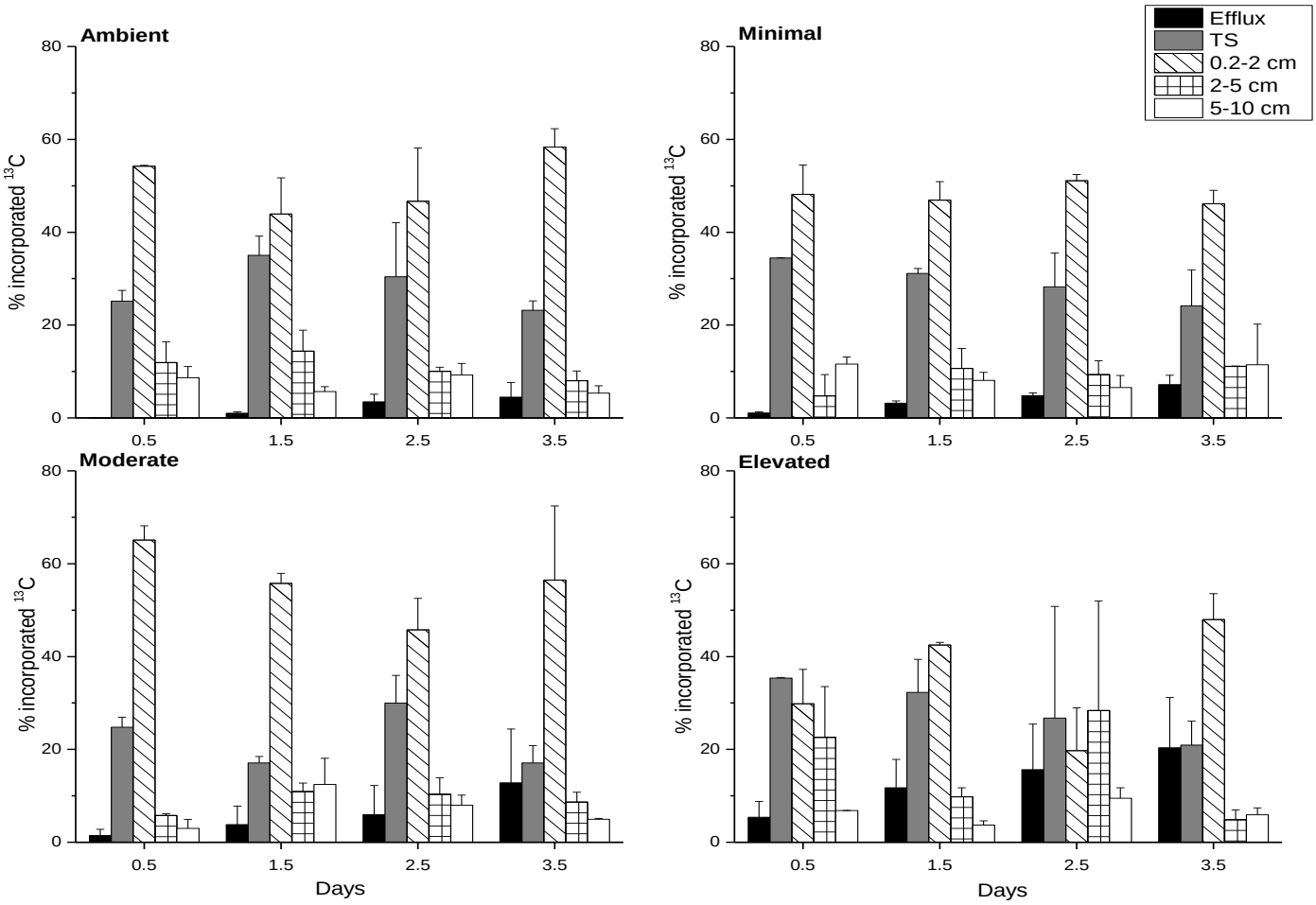

976

977 **Figure 2:** Carbon budget for excess ^{13}C within sediment OC at top scrape (TS), 0.2 to 2 cm, 2
978 to 5 cm, 5-10 cm, and the cumulative excess ^{13}C exported to the water column via the
979 combined efflux of DIC and DOC for each treatment at each sampling time. All values are as
980 a percentage of the ^{13}C initially incorporated into sediment OC (0-10 cm). Some error bars are
981 too small to be seen (mean ± SE).

982

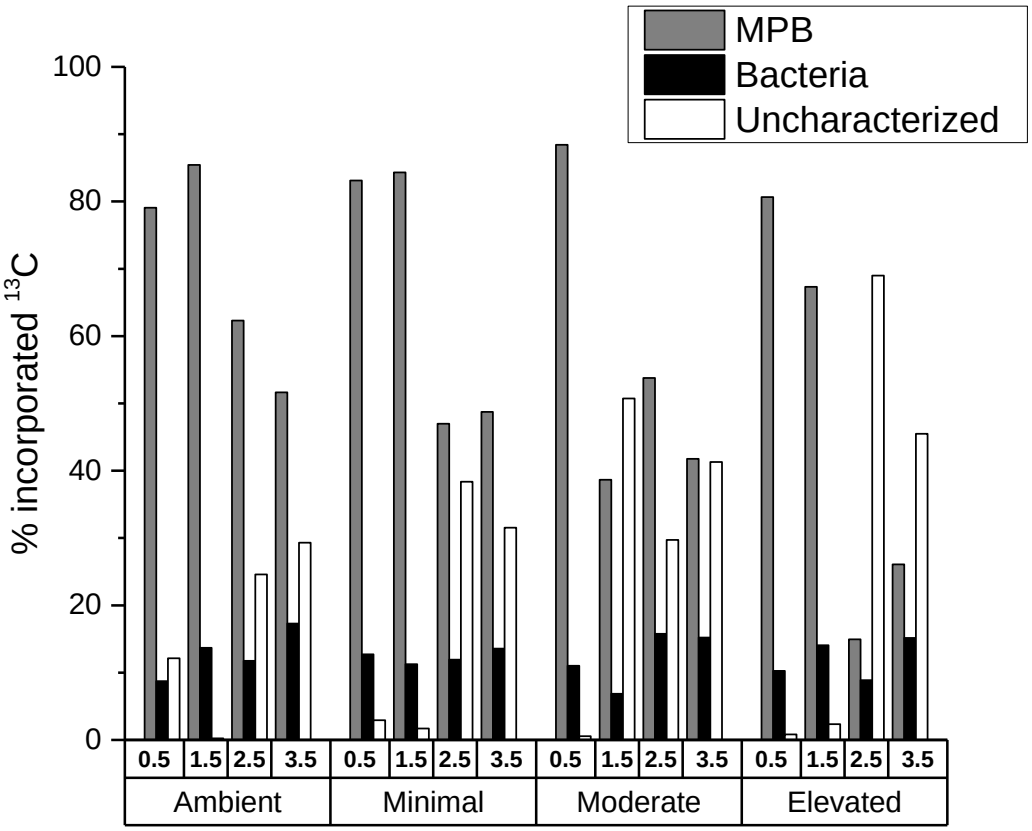

983

984 **Figure 3:** Excess ^{13}C incorporation into microphytobenthos, bacteria, and uncharacterized OC

985 as a percentage of ^{13}C contained in sediment OC in 0-10 cm. There are no error bars as PLFAs

986 were analyzed for only one replicate sample from each time period.

987

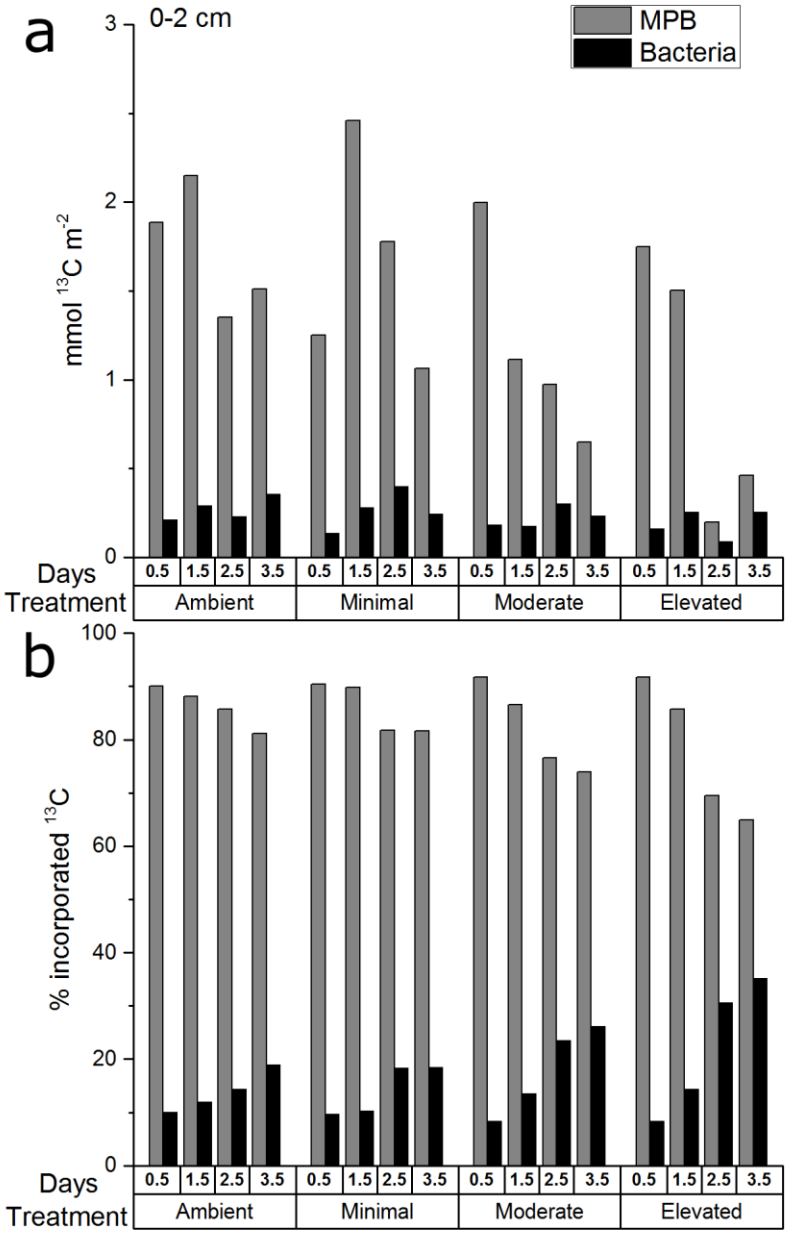

988

989 **Figure 4:** ^{13}C within MPB and bacterial biomass in sediment at 0-2 cm depth as A) total

990 excess ^{13}C (mmol ^{13}C m^{-2}) and B) a percentage of the total ^{13}C in microbial biomass at 0-2 cm

991 at each time period. There are no error bars as PLFAs were analyzed for only one replicate

992 sample from each time period.

993

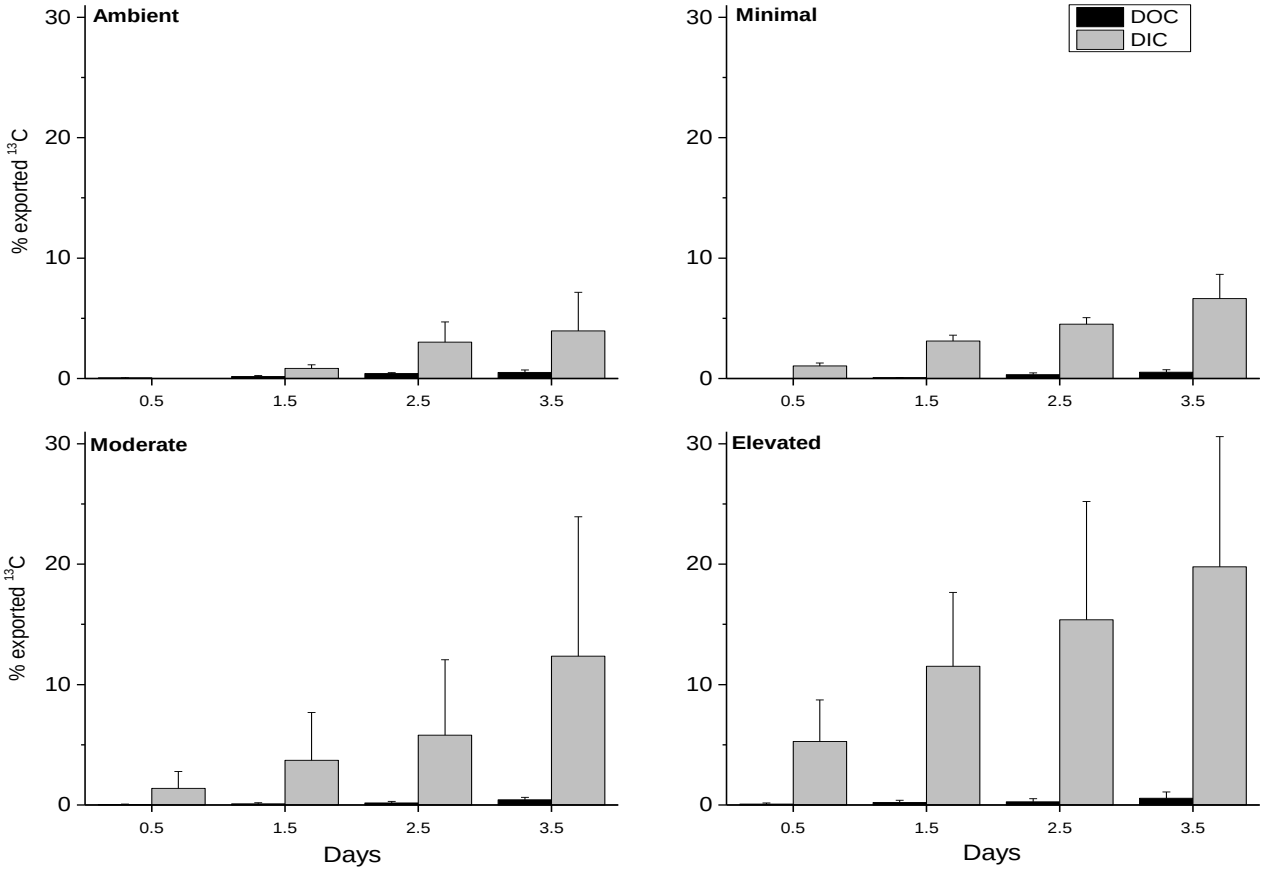

994

995 **Figure 5**: Effluxes of ^{13}C from the sediment as dissolved organic carbon (DOC) and dissolved

996 inorganic carbon (DIC) as a percentage of the total ^{13}C contained in sediment at 0-10 cm

997 depth at each sampling time (mean ± SE).

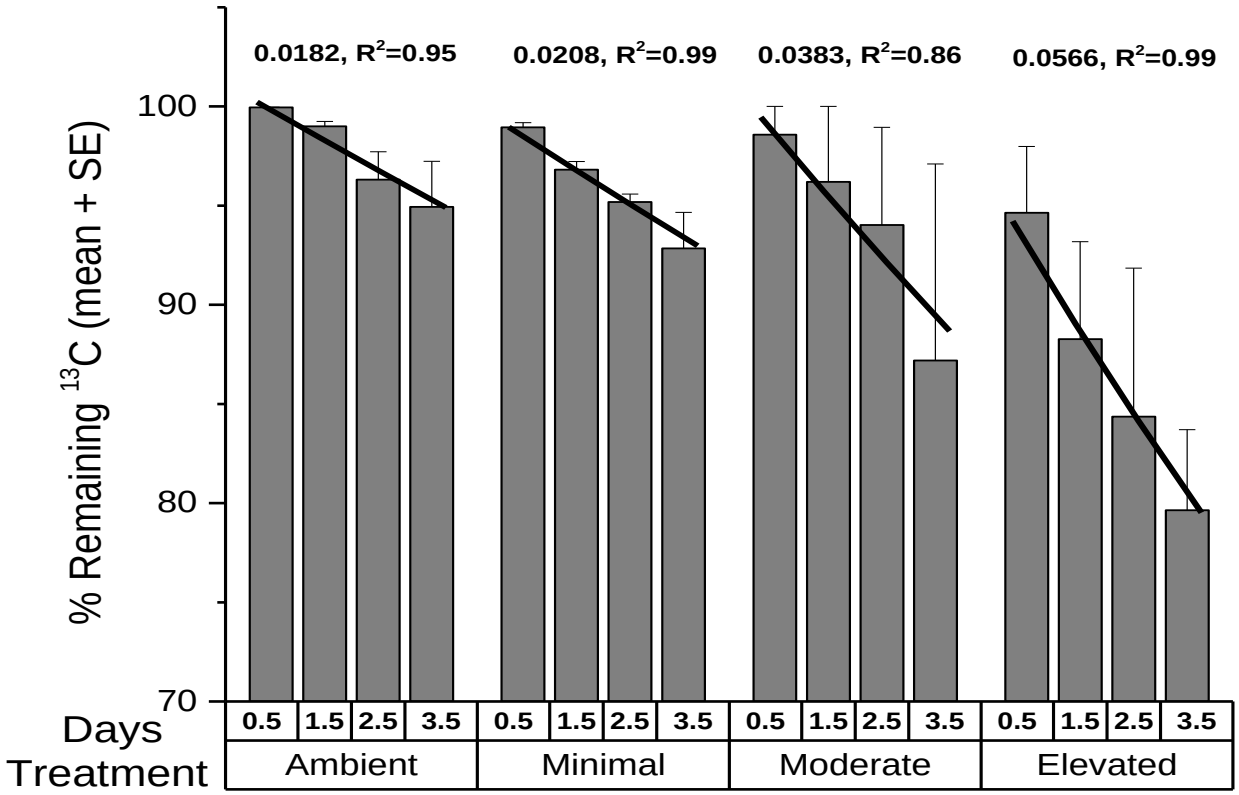

998

999 **Figure 6**: The percentage of ^{13}C remaining in sediment OC (0-10 cm depth; mean ± SE) from

1000 the calculated budget for total ^{13}C. Lines are exponential decay functions for each treatment

1001 across the 3.5 d of incubation (Loss rate constant, R^2 of function).

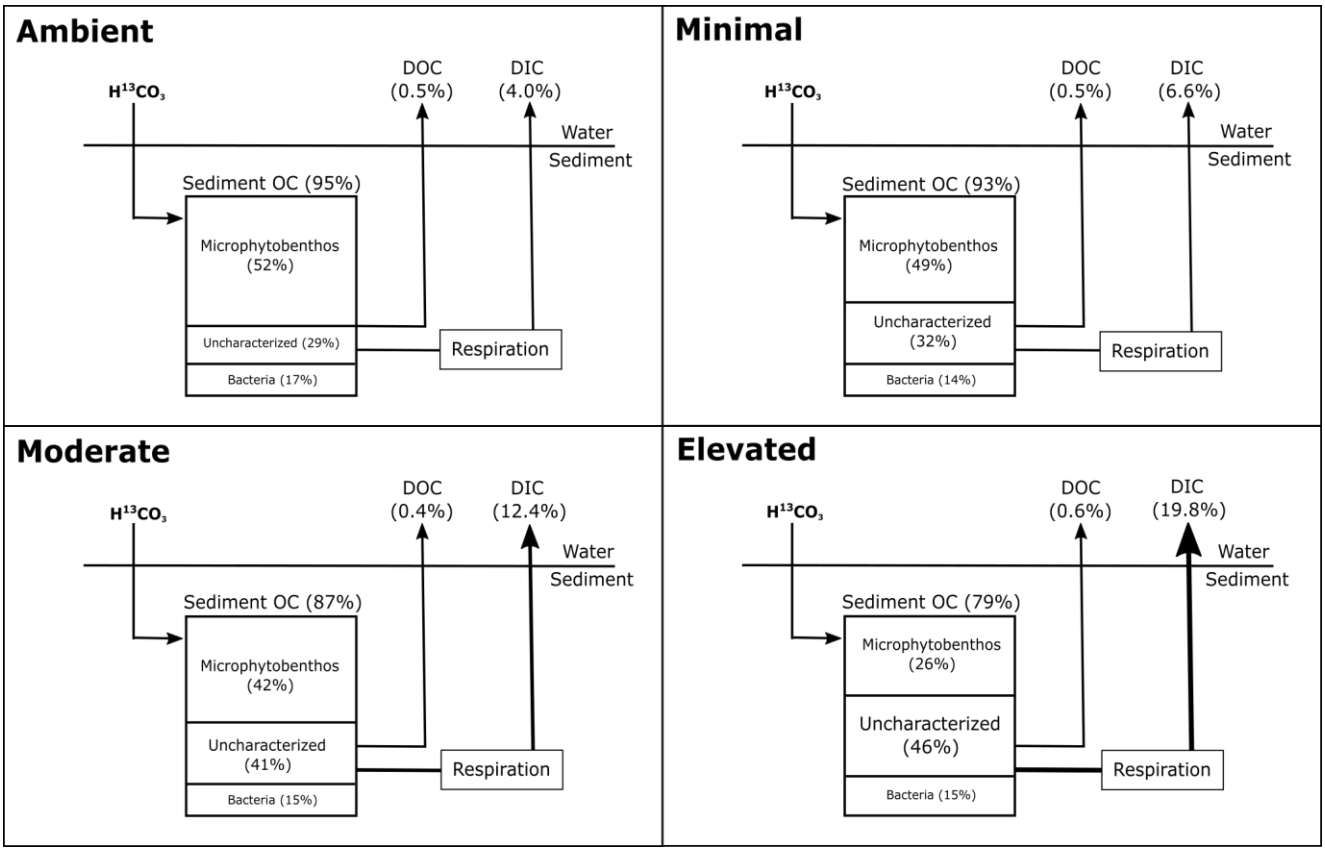

Figure 7: Distribution of ^{13}C at 3.5 d of incubation of inundated sediment including loss pathways for DIC and DOC. The ^{13}C contained in sediment organic carbon (sediment OC) is further partitioned into microphytobenthos, bacteria, and uncharacterized organic carbon as a percentage of the ^{13}C in sediment organic carbon at 0-10 cm 3.5 d after labeling (Figure layout from Eyre et al., 2016).